SOCIETY OF PETROLEUM ENGINEERS OF AIME
6300 North Central Expressway
Dallas, Texas

PAPER NUMBER SPE 835

THIS IS A PREPRINT --- SUBJECT TO CORRECTION

EFFECT OF FLUID INFLUX ON DRAWDOWN BEHAVIOR

By

H. K. Van Poolen, Member AIME, and W. J. Kunzman, Marathon Oil Co., Littleton, Colo.

ABSTRACT

Anomalous behavior shown by certain gas wells during drawdown testing and some oil fields produced by the depletion type mechanism has been successfully simulated. The combined study involved laboratory experiments and an analog computer model.

The laboratory and computer models were designed to simulate drawdown behavior of gas wells in which the pressure suddenly increases at a constant production rate following a period of pressure decline. In some oil fields produced by depletion type mechanism, this type of behavior is characterized by a sudden increase in production during the early life of the field, following a history of steady production decline where well patterns and pumping conditions are maintained constant.

In this study, the following hypothesis is proposed to explain such anomalous behavior: Hydrocarbons are concentrated in permeable lenses which are separated by tight water-bearing formations. During normal production from a downstream lens, the pressure differential between lenses becomes large enough to overcome the entry pressure of the water-bearing formations with respect to the hydrocarbons present. When the entry pressure is overcome, communication exists between lenses. The result is a sudden release of energy from an upstream lens to a downstream lens.

During a period of drawdown testing on a downstream lens, this additional source of energy could cause the pressure humps observed on some tests. In oil fields produced by the depletion type mechanism, the additional energy would cause the production humps occasionally observed. It is possible that relative permeability effects may contribute to this anomalous behavior.

References and illustrations at end of paper.

INTRODUCTION

During drawdown testing, a well is usually produced at a constant rate. Normally, pressures will monotonically decline. This decline depends on fluid characteristics, reservoir rock characteristics, and reservoir geometry and will vary for different reservoirs.

During drawdown tests of certain gas wells, operators observed that pressures would increase again with continued constant production rates. Fig. 1 shows the difference between normal and the anomalous drawdown behavior. Anomalous pressure drawdown curves are shown in Figs. 2 and 3. These tests were performed on a gas well. Table 1 summarizes the important data describing the drawdown anomalies. The producing rate of the test is given with the time of occurrence and pressure level of the minimum pressure prior to increase in pressure.

The subject formation has a limestone and shale lithology with production from porous limestone stringers which are usually less than 10 ft thick. Reservoir limits are usually determined by permeability pinchouts rather than structure. Reservoirs in the area are without a water drive.

No faults are present within 1-1/2 miles.

The literature[1] gives examples of similar behavior. Fig. 4 is one example. The phenomenon was explained by the presence of a non-sealing fault. No flow takes place across such a fault until the "radius of drainage reaches the fault".

A different explanation is suggested in this report. Fig. 5 is an artist's sketch of a well completed in a permeable lens, A. Lens A is separated from a second permeable lens, B, by a tight formation. It is assumed that both lenses and tight formations are preferentially water-wet. Only Lenses A and B contain gas. When the well is produced, the pressure will drop in Lens A. No gas will flow from Lens B to Lens A until the entry pressure of the tight formation is overcome. This occurs when the pressure of Lens A has decreased to the pressure in Lens B less the entry pressure. Thereafter, communication is established between the two lenses and an additional source of energy has become connected with the well.

The present paper describes laboratory experiments designed to simulate the process indicated in Fig. 5. A physical laboratory model was built to study the fundamentals of the process. Next, an analog model was built to further study the fundamentals of the process. Next, an analog model was built to further study the anomalous behavior using the concept of entry pressure and consideration effective permeabilities in the formation separating the lenses.

EXPERIMENTAL

A flow diagram of the laboratory apparatus is shown in Fig. 6. The main pieces of equipment are the upstream and downstream air tanks, G and I; the water saturated core, H, separating the two air tanks; the constant downstream flow regulator, J; and rotometer, K. The rotometer is used to meter the downstream flow. Pressures are monitored in the upstream and downstream air tanks by means of pressure transducers, B and D. A record of pressure vs time for upstream and downstream pressures is maintained on chart recorders, C and E. The system is charged initially to an air pressure of 90 psi by means of the air source at F.

The total upstream capacity which includes the volume of the upstream air tank and tubing lines is 497 cc. During a laboratory run, Valve L is closed and separates the upstream flow system from the downstream flow system. The total downstream capacity, which includes the volume of the downstream air tank and tubing lines, is 80 cc. The water saturated core is a Berea sandstone core with an absolute air permeability of 190 md.

A constant withdrawal rate is initiated in the downstream reservoir. The downstream reservoir is depleted until the pressure drop across the core is sufficient to overcome the entry pressure in the core. Breakthrough occurs shortly thereafter, and the two reservoirs are in communication. The two reservoirs are then depleted simultaneously through the downstream reservoir outlet.

Runs 1, 2 and 3 were obtained for a downstream reservoir flow rate of 3.40×10^{-3} cu ft/min, measured at 75F and 12 psia. For Run 4, the downstream flow rate was 5.07×10^{-3} cu ft/min, and for Run 5, the flow rate was 1.35×10^{-3} cu ft/min. Fig. 7 shows typical data as a plot of upstream reservoir pressure and downstream reservoir pressure vs time.

The effective core permeability to gas as a function of time is described by the curve labeled, "Core Permeability Function", in Fig. 7. For this curve, the function is plotted as $C\,k/\mu$, $ft^3/[min][psi]$ vs time. The function, $C\,k/\mu$, represents a form of Darcy's Law for linear flow, and is expressed as

$$C\frac{k}{\mu} = \frac{q_a}{p_2 - p_1} \quad \ldots\ldots\ldots\ldots\ldots [1]$$

where C = a constant, including core length, cross-sectional area, and a conversion factor from metric to English units,
k = permeability in millidarcies,
μ = gas viscosity in centipoise,
q_a = gas withdrawal rate from upstream reservoir measured at average core inlet and outlet pressure and 75F, and
$p_2 - p_1$ = pressure differential across core in psi.

Values for Eq. 1 are determined by material balance calculations around the upstream reservoir at any time.

ANALOG MODEL

The laboratory model was simulated on an analog computer. Certain reservoir parameters were varied to study tolerances on the pressure data. In the computer model, small changes were imposed on such parameters as original pressure, capacity of the upstream and downstream reservoirs, downstream withdrawal rate, and magnitude of the effective permeability across the water-saturated core. The computer tolerance studied showed the laboratory measurements were sufficiently accurate.

COMPUTER DIAGRAM

From a material balance around the upstream and downstream reservoirs at any time, t, the following relationships can be developed.

For the upstream reservoir,

$$\frac{dp}{dt} = \dot{p}_2 = \frac{-p_{02}q_2}{q_2} \quad \ldots\ldots\ldots\ldots [2]$$

where $\dot{p}_2$ = change in pressure with respect to time in the upstream reservoir,
p_{02} = initial pressure in the upstream reservoir in psia,
q_2 = withdrawal rate from the upstream reservoir at 12 psia and 75F, cu ft per minute, and
Q_2 = initial volume of gas in the upstream reservoir in cu ft at 12 psia and 75F.

For the downstream reservoir,

$$\dot{p}_1 = \frac{-p_{01}}{Q_1}(q_1 - q_2) \quad \ldots\ldots\ldots [3]$$

where $\dot{p}_1$ = change in pressure with respect to time in the downstream reservoir,
p_{01} = initial pressure in the downstream reservoir in psia,
Q_1 = initial volume of gas in downstream reservoir at 12 psia and 75F, and
q_1 = gas withdrawal rate from the downstream reservoir at 12 psia and 75F, cu ft/min.

Eqs. 2 and 3 were used to develop a schematic diagram for the analog simulation of the laboratory model. The schematic diagram of the analog computer hook-up is shown in Fig. 8.

COMPUTER RESULTS

In a series of computer runs, upstream reservoir pressure, downstream reservoir pressure, and the function, C k/μ, were plotted vs time in minutes. Laboratory Runs 1, 2 and 3 were simulated on the analog computer. The curve describing C k/μ vs time was set up on variable function generators for each run. The analog simulation of Laboratory Run 1 is shown in Fig. 7. The computer curves corresponding to upstream and downstream reservoir pressure vs time are shown as dashed lines for comparison. The curve describing C k/μ vs time represents laboratory data only, since the computer simulation was identical with laboratory data for corresponding runs.

Tolerance effects in the pressure drawdown curves were studied in the computer simulation by variation of C k/μ, q_1, p_2/Q_2, p_1/Q_1 and p_o. In Fig. 9, the curves labeled A represent a simulation of Laboratory Run 2. In Case B, the time of initial breakthrough was delayed from one minute to four minutes. The resulting effect on the drawdown curves is shown. In Fig. 10, a change in the magnitude for C k/μ is shown for Laboratory Run 3. In this figure, the curves labeled B represent a simulation of Laboratory Run 3. The effect can be seen in the shifted drawdown curves.

The computer study appears to show that delaying the initial time of breakthrough causes more severe humping on the downstream drawdown curve. The humping also occurs later as the initial breakthrough is delayed [see Fig. 9]. As the magnitude of the permeability function C k/μ, is increased, an increase in the humping is observed [see Fig. 10]. The computer study showed that the pressure data were little affected by small changes in the parameters, q_1, p_2/Q_2, p_1/Q_1 and p_o. These results show the laboratory measurements were sufficiently accurate.

DISCUSSION OF RESULTS

The laboratory tests definitely exhibited humping drawdown behavior. The pressure in the upstream cylinder remained constant for some time, indicating no flow across the water-saturated core. Following some time of constant rate withdrawal, the pressure in the downstream cell reduced sufficiently to cause a large enough pressure drop across the water-saturated core to initiate flow.

Table 2 shows pressure drops across the core at the time flow started from the upstream cylinder. Fair repeatability exists for the rate of 3.4×10^{-3} cu ft/min. Data for Run 3 may be off, because of a different saturation technique for this run.

The analog computer runs have indicated that the data obtained in the laboratory is of sufficient accuracy. If displacement data on cores are available, the analog computer could be used to simulate the laboratory data. The computer study showed the significance of the C k/μ curves in affecting the shape of the drawdown curves. An increase in the magnitude of the C k/μ curves and a delay in time of initial breakthrough cause more severe humping in the drawdown curves.

The observed drawdown behavior may be the result of entry pressure, relative permeability effects, or both. The present tests do not allow differentiation between these causes. That the observed field behavior is repeatable may mean relative permeability is more important than entry pressure.

An interesting note is that humping drawdowns have been observed on gas wells only. This limitation may be due to the repeatability one may get on gas wells and not on oil wells. It might be that water saturations may be more readily re-established in the presence of gas than in the presence of oil.

DELAYED ENERGY IN DEPLETION DRIVES

Fields which produce by the depletion mechanism should show a steady production decline if well patterns and pumping conditions are maintained constant. Some fields deviate from this behavior by a sudden increase in production during the later life. One example is the Downer

Field in Banner County, Nebraska, Denver Julesberg Basin.[2]

The field is located in an area dominated by regional dip, and structural factors have little influence on the oil entrapment. The productive D sands are near 5,800 ft. Although the Downer producing area is classified as one field, the locations of the dry holes and producing wells point out that production is obtained from several sand lenses within the D interval. The lenses are apparently individual stratigraphic traps separated by gradational permeability variations. Correlation of logs indicates that the four subject wells drain an apparently common reservoir.

The producing sands are of medium quality and range in thickness from 4 to 12 ft. Porosities vary from 16.5 to 19.6 per cent with permeabilities in the 25 to 100 md range. All wells were fractured on completion. The crude oil is 37° API gravity and originally contained an estimated 700 cu ft of gas in solution per barrel. The original reservoir pressure was near 1,500 psi.

The Downer Field wells were drilled during 1955. Initial producing rates ranged generally from 100 to 300 BOPD. None of these wells produced more than a trace of water initially. No significant saturation changes nor indication of a water table were noted.

Producing history for the field is shown in Fig. 11. The productivity decline to early 1958 is normal for solution gas drive production. After that time, the productivity shows a marked and continuous increase for approximately two years. The production increase was followed by a normal decline. In late 1961, one well was added as a water injection well, and in mid-1962, one producer was converted to an injection well. Production did not increase until late 1962.

The sudden increase in productivity is explained by later communication of oil-containing lenses originally separated by water-bearing tighter lenses. The communication and its corresponding release of energy from the lenses is the result of overcoming capillary entry pressures between lenses and tight water-bearing rocks. A similar explanation can be given to the delayed response from water injection.

PREFERENTIAL DRAINAGE

A relatively common occurrence is the proportionately high recovery noted[2] from discovery wells in some fields. Due to the initial reduction in pressure in the area of the initial well, the lenses become connected with the well. Later wells would have to reduce their pressure considerably before entry pressure is overcome.

CONCLUSIONS

In gas wells, anomalous increases in pressure with continued production have been observed. At least one field has shown an increase in production at pumped-off conditions without the addition of external energy such as a water drive.

This report is written around the following hypothesis: Hydrocarbons are concentrated in permeable lenses which are surrounded by tight water-bearing formations. When the pressure differential between lenses becomes sufficiently large, the entry pressure of the tight water-bearing formation with respect to the hydrocarbons present is overcome. When the entry pressure is surpassed, communication exists between the lenses. Regarding the downstream pressure lens, such sudden communication is equivalent to increased energy connection.

A laboratory model was constructed to simulate the "humping" behavior. Pressure humps are observed on the tests. These humps could be caused by entry pressure combined with relative permeability in the water-saturated core separating two pressure vessels or the relative permeability effects alone.

An analog study was made to simulate the laboratory model. Good agreement was obtained, and the accuracy of the laboratory data was established.

NOMENCLATURE

p_1 = downstream reservoir pressure, lb/sq in.
p_2 = upstream reservoir pressure, lb/sq in.
p_{01} = initial pressure in downstream reservoir, lb/sq in.
p_{02} = initial pressure in upstream reservoir, lb/sq in.
$\dot{p}_1$ = pressure change with respect to time in downstream reservoir, lb/[sq in.][min]
$\dot{p}_2$ = pressure change with respect to time in upstream reservoir, lb/[sq in.][min]
*Q_1 = initial volume of gas in downstream reservoir, cu ft
*Q_2 = initial volume of gas in upstream reservoir cu ft
*q_1 = gas withdrawal rate from downstream reservoir, cu ft/min
*q_2 = gas withdrawal rate from upstream reservoir during time interval, Δt, cu ft/min
*q_a = gas withdrawal rate from upstream reservoir measured at average core inlet and outlet pressure, cu ft/min
C = a constant, including core length, cross-sectional area, and conversion factor from metric to English units, $\frac{[cp][cu\ ft][sq\ in.]}{[lb][md][min]}$
μ = gas viscosity, centipoise

*Volumes measured at standard conditions of 12 psia and 75 F.

REFERENCES

1. Jones, Park: "Reservoir Limit Test on Gas Wells", Jour. Pet. Tech. [June, 1962] 613.

2. Kirchmann, Frank: "Delayed Water Drive and Preferential Drainage", Term paper, Colorado School of Mines, Fall 1960.

TABLE 1

SUMMARY OF DRAWDOWN ANOMALIES IN A GAS WELL (ZONES A AND B)

Zone	q = MCF/day	Minimum Value in Drawdown Curve	
		Time hr	Surface Pressure $(psia)^2$
Zone A	870	0.5	6,700,000
Zone A	1072	0.7	6,100,000
Zone B*	1567	0.25	8,156,000
Zone B**	2006	0.24	7,340,000

* See Figure 2.

**See Figure 3.

TABLE 2

PRESSURE DIFFERENTIALS ACROSS CORES AT TIMES WHEN FLOW THROUGH CORE STARTS

Run No.	downstream flow rate x 10^3 ft^3/min	t, time flow started across core, min	cumulative downstream effluent, $ft^3 \times 10^3$ at t	Δp, pressure differential across core at t, psi
1	3.4	1.0	3.4	19.2
2	3.4	1.0	3.4	23.1
3	3.4	1.5	5.1	26.0
4	5.07	0.5	2.5	15.7
5	1.35	1.5	2.0	12.3

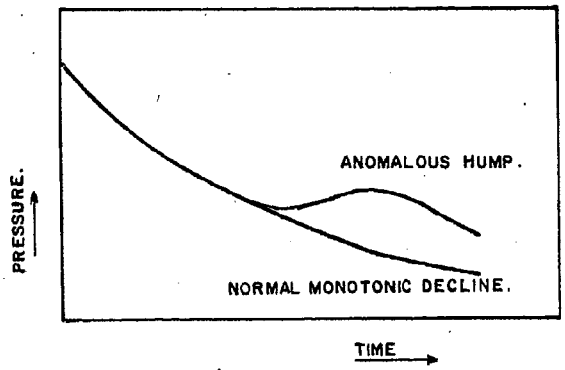

Fig. 1 - Drawdown Behavior at Constant Producing Rate

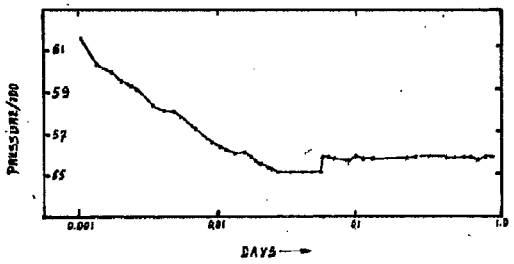

Fig. 4 - Well Near a Non-Sealing Fault

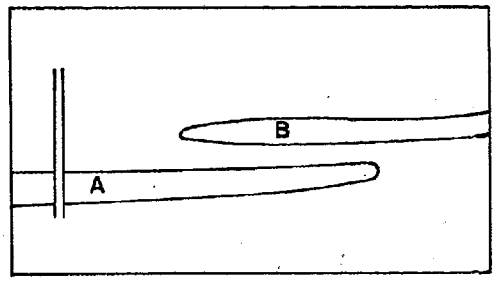

Fig. 5 - Artist's Sketch of Lenticular Formation

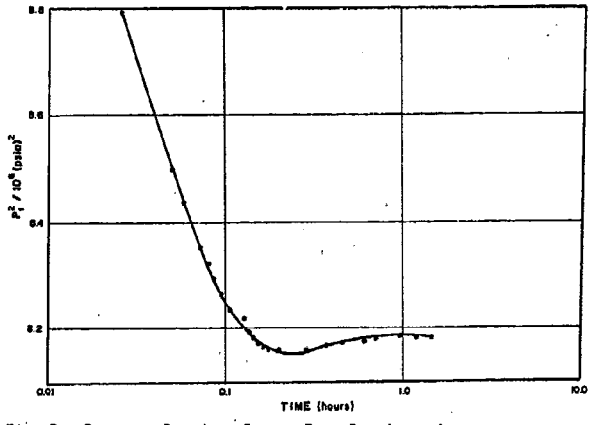

Fig. 2 - Pressure Drawdown Curve, Zone B, 4th Rate, q = 1567 MCF/D; (Surface Pressure)^2 Versus Log of Time

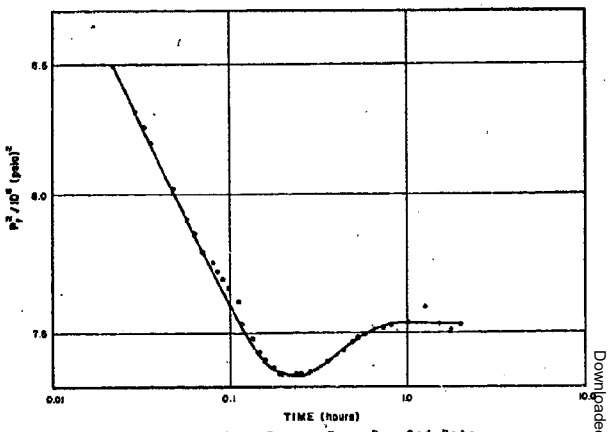

Fig. 3 - Pressure Drawdown Curve, Zone B, 3rd Rate, q= 2006 MCF/D; (Flowing Surface Pressure)^2 Versus Log of Time.

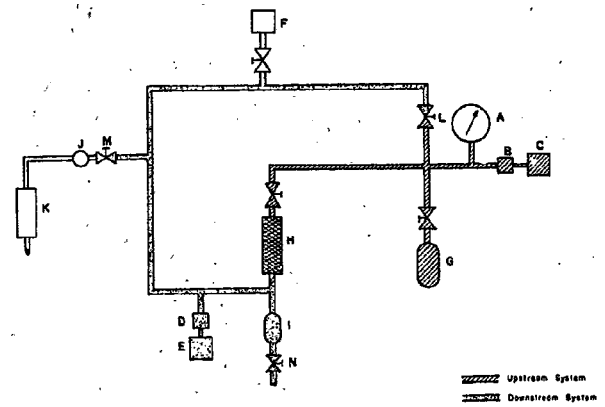

Fig. 6 - Flow Diagram of Laboratory Apparatus for Humping Drawdown. A-pressure Gauge; B-0-400 Psia Pressure Transducer; C-10 MV Recorder; D-0-400 Psia Pressure Transducer; E-10 MV Recorder; F-90 Psi Air Source; G-Upstream Air Tank; H-Water Saturated Core I-Downstream Air Tank; J-Constant Flow Regulator; K-Rotometer; L,M,N-Line Valves.

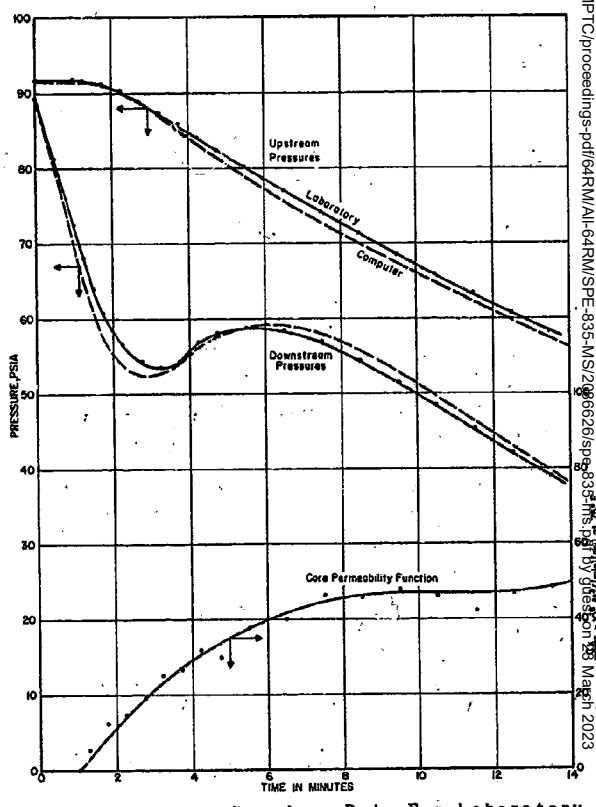

Fig. 7 - Humping Drawdown Data For Laboratory Run No. 1

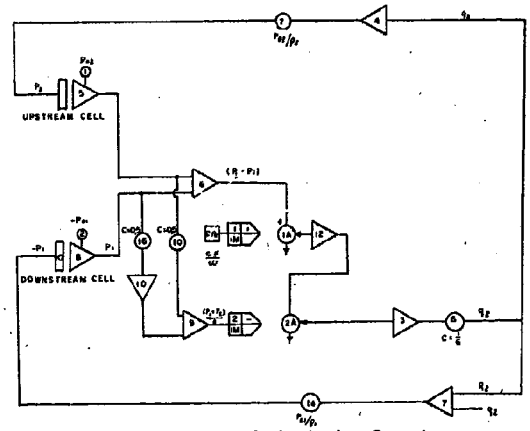

Fig. 8 - Schematic Diagram of the Analog Computer Hook-Up

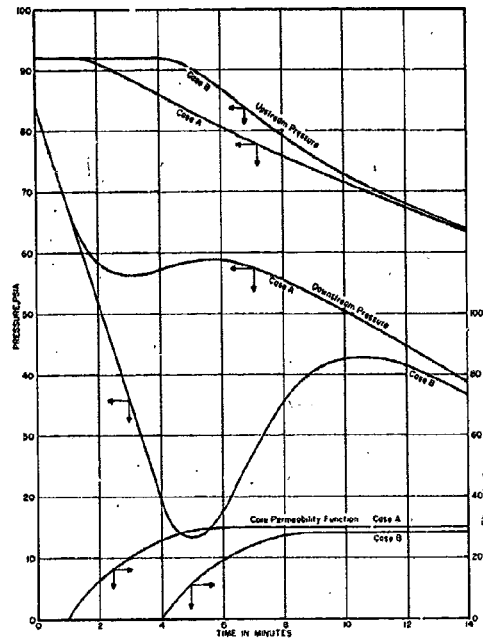

Fig. 9 - Analog Simulation of Laboratory Run No. 2 Showing Shifted Permeability Function

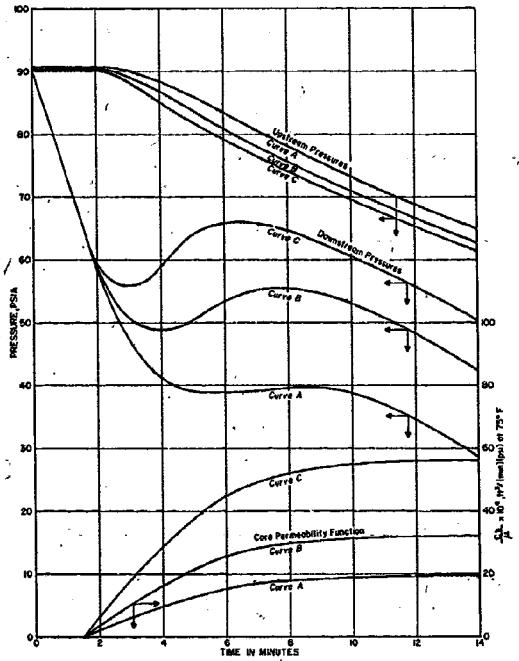

Fig. 10 - Analog Simulator of Laboratory Run No. 3 For Variable Permeability Across Core

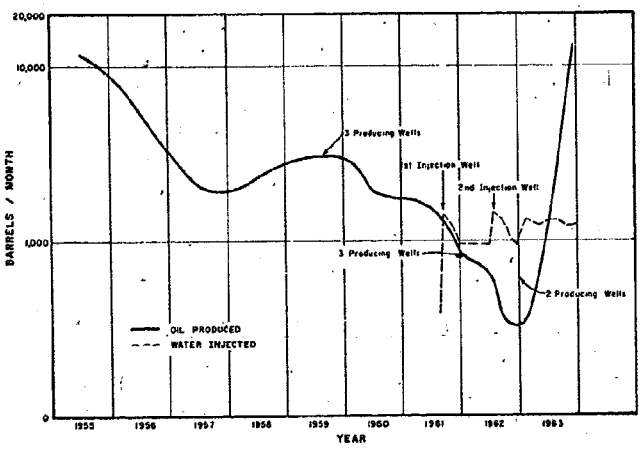

Fig. 11 - Production History, Downer Field, Banner County, Nebraska